Available online at www.sciencedirect.com
SCIENCE DIRECT®
Thermochimica Acta 416 (2004) 121–127
thermochimica acta
www.elsevier.com/locate/tca

Liquid crystallization of glassy guar gum with water☆

Tatsuko Hatakeyama[a,*], Sunao Naoi[a], Hyoe Hatakeyama[b,1]

[a] *Otsuma Women's University, 12, Sanban-cho, Chiyoda-ku, Tokyo 102-8357, Japan*
[b] *Fukui University of Technology, 3-6-1 Gakuen, Fukui 910-8505, Japan*

Received 1 November 2002; received in revised form 5 February 2003; accepted 10 February 2003

Available online 4 February 2004

Abstract

Liquid crystal formation of guar gum (GG) in the presence of water was investigated by differential scanning calorimetry. GG is a neutral galactomannan, consists of 1,4-β-D-mannose backbone and 1,6-α-D-galactose side chains, and the galactose/mannose ratio is 1:2. It was found that GG–water has a specific water content range where the liquid crystallization takes place. When GG–non-freezing water system is solidified rapidly, it was frozen into the glassy state. By heating, glass transition, cold crystallization and liquid crystallization are observed. Liquid crystallization took place at cold crystallization. By slow cooling, a part of GG molecules associated with water is liquid crystallized on cooling and the rest amount is frozen in the glassy state. Glassy region forms liquid crystal which is observed as the cold crystallization. The summation of enthalpy of liquid crystallization obtained on cooling and that of cold crystallization on heating accords well with that of transition from liquid crystal to isotropic liquid.

Keywords: Guar gum; Water; Phase transition; DSC; Glass transition

1. Introduction

Guar gum (GG) is a member of the galactomannan family [1,2] consisting of 1,4-β-D-mannose backbone and 1,6-α-D-galactose side chains, and the galactose/mannose ratio is 1:2. GG has been paid particular attention as an industrial polysaccharide due to its rheological properties [3,4]. GG has been mixed with various kinds of polysaccharides, such as carrageenan [5,6] and xanthan gum [7], in order to control viscoelastic properties. At the same time, it is known that GG–polysaccharide mixtures form hydrogels when they are cross-linked by borate [8–10].

We have reported the phase transition of neutral galactomannan, such as locust bean gum (LBG)–, tara gum (Tara-G)–, and guar gum–water systems having various water contents [11]. These three galactomannan samples have different number of side chains in the repeating unit of the main chain. The three galactomannan samples consist of 1,4-β-D-mannose backbone and 1,6-α-D-galactose side chains, and the galactose/mannose ratio is 1:4, 1:3 and 1:2 for LBG, Tara-G and GG, respectively. Among the above three galactomannan, it was found that GG showed a specific thermal behaviour [11].

Phase transition behaviour of polysaccharide–water systems has been reported, however, the majority of reports are concerned with polysaccharide electrolyte–water systems [12–16]. In our previous report [11], phase transition behaviour of galactomannan–water systems has been investigated in a water content ($=W_c$) = (mass of water)/(mass of dry sample), ($g\,g^{-1}$) range from 0 to ca. 5.0 $g\,g^{-1}$ by differential scanning calorimetry (DSC). In heating DSC curves for three types of galactomannan–water systems, glass transition, cold crystallization, and melting of water were observed. The effect of chemical structure was clearly found in a water content range where glass transition and cold crystallization were observed. The temperature range showing glass transition and cold crystallization increased according to the order of side chain number, i.e. the W_c range of LBG–water systems was from 0.6 to 0.7, Tara-G–water systems from 0.6 to 1.0 and GG–water systems from 0.4 to 2.7 $g\,g^{-1}$. This indicates that the glassy state of GG–water systems is formed in a wider

☆ Presented at the Third International and Fifth China–Japan Joint Symposium on Calorimetry and Thermal Analysis held in Lanzhou, China, 15–18 August 2002.

* Corresponding author. Tel.: +81-3-5275-6023; fax: +81-3-5275-6932.
E-mail address: hatakeyama@otsuma.ac.jp (T. Hatakeyama).
[1] Tel.: +81-776-22-811; fax: +81-776-22-7891.

0040-6031/$ – see front matter © 2003 Elsevier B.V. All rights reserved.
doi:10.1016/j.tca.2003.02.003

W_c range than that of LBG– and Tara-G–water systems. Furthermore, in addition glass transition, cold crystallization and melting, transition from liquid crystal to isotropic liquid was observed in GG–water systems at about 20 °C in a water content ranging from 0.4 to 2.7 g g^{-1}. It is considered that water–galactomannan interaction is affected by chemical structure and that the structural change of water markedly influences the phase behaviour.

In order to understand the structural change of water, the amount of bound water content was calculated based on the enthalpy of melting of water in the systems. Water molecules coexisting with polysaccharides are categorized into three types, such as, free water (W_f), freezing bound water (W_{fb}), and non-freezing water (W_{nf}). The characteristic of each type of water is that melting of W_f starts at 0 °C, W_{fb} lower than 0 °C, and W_{nf} shows no first-order transition [17]. It was found that LBG having a low side chain number has the largest amount of W_{nf}, and GG having the highest side chain number has the lowest amount of W_{fb}. In our previous report, it was found that LBG–water systems formed gels by freezing and thawing process [18,19], and GG–water systems formed liquid crystals. It is considered that the amount of W_{nf} and W_{fb} relates to the gelation and liquid crystallization. It has been reported that liquid crystals of polysaccharide electrolyte–water systems [12–16] show both thermotropic and lyotropic characteristic features [20].

In this study, the aim is to investigate the liquid crystalline properties of GG–water systems, which are an example of neutral polysaccharide–water systems, in relation to the structural change of water in saccharides.

2. Experimental

Guar gum was provided by Fuso Kagaku Co. Ltd., Japan, and the commercial name is DKS Fine Gum G-270. The chemical structure of GG is shown in Fig. 1.

A Seiko Instruments Ltd. differential scanning calorimeter DSC200C equipped with a cooling apparatus was used. Nitrogen gas flow rate was 20 ml min^{-1}. Aluminium sealed type pans were weighed by Sartorius micro-balance with precision $\pm 0.1 \times 10^{-7}$ g. Samples about 3–5 mg were placed in the pans and a small amount of water was added using a micro-syringe. The water was evaporated until an appropriate amount of water was attained. Then, the sample pans were sealed hermetically using an auto-sealer. Samples with added water were weighed. Samples were kept at room temperature overnight in order to confirm that no mass loss occurred and DSC measurements were carried out. The samples were heated to 60 °C then, cooled to −150 °C. The samples were held at −150 °C for 10 min, and heated to 60 °C. Cooling rates were 1–50 °C min^{-1}, and heating rate was 10 °C min^{-1}. The pans were pierced after DSC measurement, and then were annealed at 120 °C for over 1 h in an electric oven. Water content (W_c) was defined by the following equation:

$$\text{Water content } (W_c) = \frac{\text{mass of water}}{\text{mass of dry sample}} \ (\text{g g}^{-1}) \quad (1)$$

Glass transition temperature (T_g) was defined as the temperature at which the extrapolated baseline before the transition intersects the tangent drawn at the point of greatest slope on the step of the glass transition [21,22]. Temperature and enthalpy of crystallization and melting of the sample were calibrated using indium and pure water as a standard material. The heat capacity difference (ΔC_p) at T_g was calculated using the total weight of sample [11,23]. Peak temperatures were assigned as crystallization temperature (T_c), transition temperature from isotropic liquid state to liquid crystalline state in cooling (T_c^*), melting temperature (T_m), cold-crystallization temperature (T_{cc}) and transition temperature from liquid crystalline state to isotropic liquid state in heating (T_m^*), respectively. At the same time, starting temperature of melting was defined as T_{im}. In this study, cold crystallization is defined as an exothermic transition which occurs in a temperature range between T_g and T_m temperature was calibrated using pure water and starting temperature of cooling and melting were determined as 0 °C at heating rate of 10 °C min^{-1}. Crystallization enthalpy (ΔH_c), cold-crystallization enthalpy (ΔH_{Hz}) and melting peak enthalpy (ΔH_m) were calculated using mass of water in the GG–water systems. Enthalpy of liquid crystal transitions in cooling (ΔH_c^*) and heating (ΔH_m^*) were calculated using the total mass of systems. Freezing water (W_f) was evaluated using the following equation. W_f contains free water and freezing bound water (W_{fb}). Enthalpy of melting water (334 J g^{-1}) was used for calculation:

$$\text{Freezing water } (W_f) = \frac{\Delta H_m / 334}{m_{\text{dry sample}}} \quad (2)$$

where $m_{\text{dry sample}}$ is mass of dry sample. Non-freezing water was defined as follows:

$$\text{Non-freezing water } (W_{nf}) = W_c - W_f \quad (3)$$

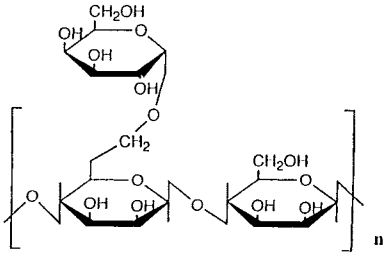

Fig. 1. Chemical structure of guar gum.

3. Results and discussion

When GG–water systems with a W_c range from 0 to 3.0 g g^{-1} were measured by DSC in a temperature range from −150 to 50 °C, heating and cooling curves of the system varied in a complex manner as a function of W_c. As

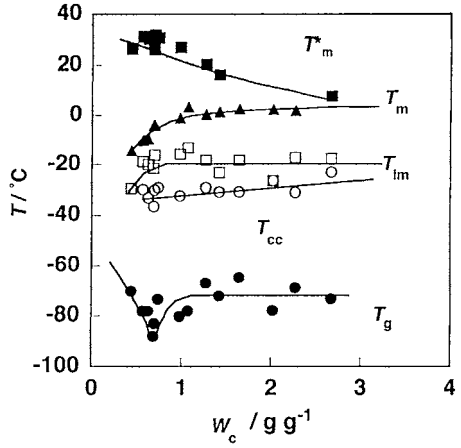

Fig. 2. Phase diagram of GG–water systems. T_g: glass transition temperature, T_{cc}: cold-crystallization temperature, T_{im}: starting temperature of melting, T_m: melting peak temperature, T^*_m: liquid crystallization temperature.

stated in the introductory section, from the low to high temperature side, glass transition, cold crystallization, melting and liquid crystallization were observed in GG–water systems. Based on DSC heating curves, the phase diagram of GG–water systems is obtained as shown in Fig. 2. Each transition temperature shown in Fig. 2 was defined as stated in Section 2. In order to investigate the liquid crystal formation of GG–water systems, three samples showing characteristic phase transition behaviour were chosen, i.e. the sample with W_c = ca. 0.6 g g^{-1} where T_g decreases as a function of W_c, the sample with W_c = 0.8 g g^{-1} where the T_g reaches the minimum, and the sample with W_c = 1.7 g g^{-1} where the transition from liquid crystal to isotropic liquid is hardly distinguished in the DSC heating curve.

Fig. 3 shows DSC cooling curves of the sample with W_c = 0.59 g g^{-1} measured at various cooling rates from 1 to 40 °C min^{-1}. Two exothermic peaks, a main peak at about −20 °C and a broad sub-peak at −50 °C, are found. The main peak is observed in cooling curves regardless of cooling rate, in contrast the sub-peak is merged into the main when cooling rate exceeds 20 °C min^{-1}. Both peaks shift to the low temperature side with increasing cooling rate.

Fig. 4 shows DSC heating curves measured at 10 °C min^{-1} of the above samples with W_c = 0.59 g g^{-1} which have been cooled at various cooling rates. As already reported in our previous paper, the amount of water (0.59 g g^{-1}) in this system corresponds to the amount of non-freezing water [11]. Glass transition is clearly observed as a baseline shift at around −70 °C. The heat capacity difference at T_g (ΔC_p) is far larger than that of ordinary amorphous polymers [24–26]. Shallow exothermic peak at around −30 °C is attributed to cold crystallization. A similar cold crystallization peak is generally observed in other polysaccharide–water systems when they are quenched from the liquid state to the glassy state [23]. Values of T_g and the starting temperature of cold crystallization shift to the low temperature

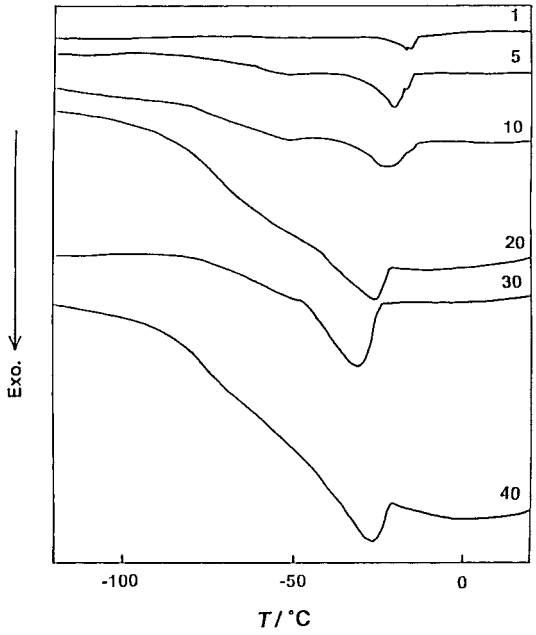

Fig. 3. Stacked DSC cooling curves of various cooling rates of the sample with W_c = 0.59 g g^{-1}. Numerals in the figure shows cooling rate.

side with increasing cooling rate. ΔH_{cc} also increases with increasing cooling rates. After the cold crystallization, two distinct endothermic peaks are observed at around −5 and 30 °C. Comparing the phase transition temperatures of other polysaccharide–water systems [12,17], a small peak is attributed to melting of ice, and a large endotherm is attributed to transition from liquid crystal to isotropic liquid. It is noted that T_m is observed at a temperature lower than 0 °C,

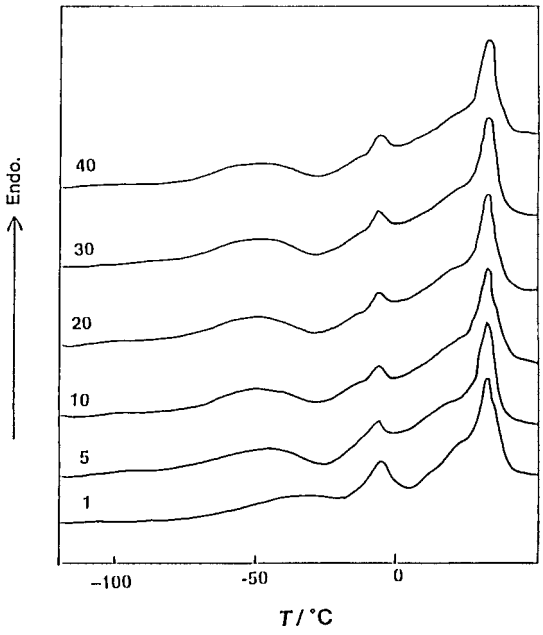

Fig. 4. Stacked DSC heating curves of the sample with W_c = 0.59 g g^{-1} cooled from 50 to −150 °C at various cooling rates. Heating rate = 10 °C min^{-1}.

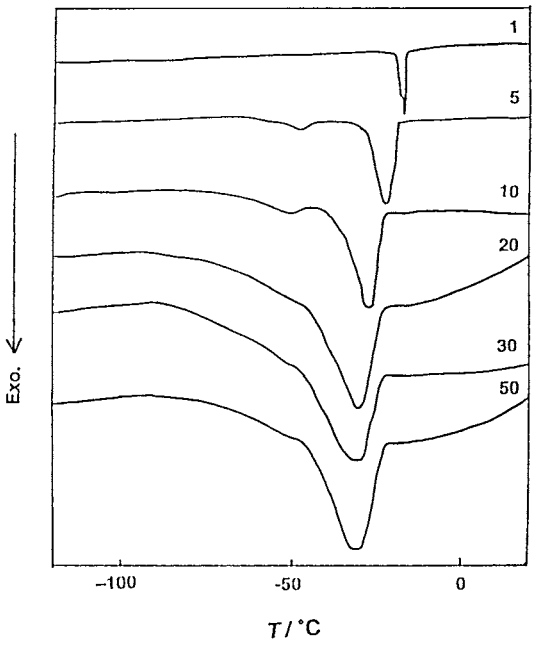

Fig. 5. Stacked DSC cooling curves of various cooling rates of the sample with $W_c = 0.81\,g\,g^{-1}$. Numerals in the figure shows cooling rate.

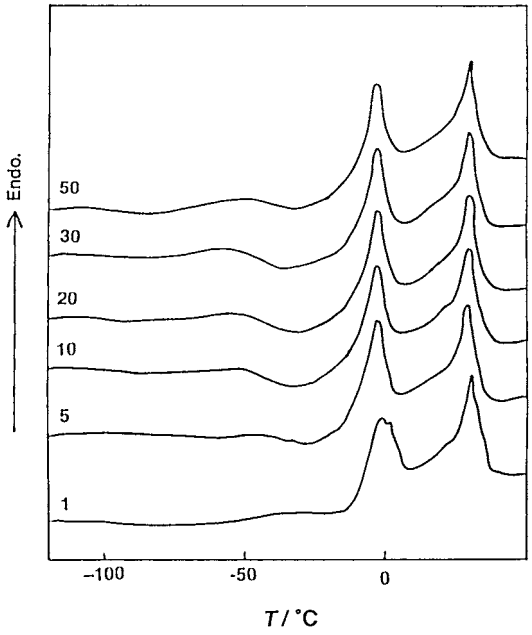

Fig. 6. Stacked DSC heating curves of the sample with $W_c = 0.81\,g\,g^{-1}$ cooled from 50 to −150 °C at various cooling rates. Heating rate = 10 °C min^{-1}.

indicating that this water is not normal free water, but freezing bound water affected by the presence of GG molecules. As clearly seen in Fig. 4, ΔH_m^* is larger than ΔH_m.

When DSC cooling curves shown in Fig. 3 are compared with those of Fig. 4, the large exothermic peak observed at ca. −20 °C in Fig. 3 is attributed to liquid crystallization. Therefore, peak temperature is designated as T_c^*. Moreover, the low temperature side exothermic peak is attributable to crystallization of freezing bound water in the system. The above DSC curves suggest that almost all water molecules in the systems are strongly restricted by GG molecules when W_c is $0.50\,g\,g^{-1}$.

Fig. 5 shows DSC cooling curves of the sample with W_c is $0.81\,g\,g^{-1}$ measured at various cooling rates. When the phase diagram shown in Fig. 2 is referred to, the sample with $W_c = 0.81\,g\,g^{-1}$ is located in the W_c range where T_g reaches the minimum point. In Fig. 5, two exothermic peaks, a main peak at around −30 °C and a broad sub-peak at around −50 °C are observed. DSC cooling curves are similar to those of the samples with $W_c = 0.59\,g\,g^{-1}$, although T_c^* of this sample is 10 °C lower than that of the sample with $W_c = 0.59\,g\,g^{-1}$. Crystallization peak of water clearly separated from liquid crystallization peak at cooling rates of 5 and 10 °C min^{-1}. Crystallization of water is recognized as a shoulder peak when cooling rate exceeds 20 °C min^{-1}. Liquid crystallization peak shifts to the low temperature side merging with crystallization peak. This is due to the fact that T_c^* depends markedly on cooling rate, in contrast, T_c maintains a constant temperature. The crystallization peak of the sample with $W_c = 0.81\,g\ g^{-1}$ is more clearly observed than that of $W_c = 0.59\,g\,g^{-1}$. ΔH_c^* of the sample with $W_c = 0.81\,g\,g^{-1}$ is larger than that of $W_c = 0.59\,g\,g^{-1}$. In both samples with W_c of 0.59 and $0.81\,g\,g^{-1}$, T_c was not detected at 1 °C min^{-1} due to the decrease of apparent sensitivity.

Fig. 6 shows DSC heating curves measured at 10 °C min^{-1} of the sample with $W_c = 0.81\,g\,g^{-1}$ having cooled at various rates. T_g at −80 °C, T_{cc} at −30 °C, T_m at about 0 °C and T_m^* at 20 °C are observed. It is clearly seen that ΔH_m^* is almost the same as ΔH_m. T_g and the starting temperature of cold crystallization shift to the low temperature side and ΔH_{cc} increases with increasing cooling rates. Cold crystallization peak of $W_c = 0.81\,g\,g^{-1}$ is broader compared with that of $W_c = 0.59\,g\,g^{-1}$. T_g of $W_c = 0.81\,g\,g^{-1}$ is lower than that of $W_c = 0.59\,g\,g^{-1}$ and ΔH_m^* of $W_c = 0.81\,g\,g^{-1}$ is smaller than that of $W_c = 0.59\,g\,g^{-1}$.

Fig. 7 shows DSC cooling curves of the sample with $W_c = 1.71\,g\,g^{-1}$ measured at various cooling rates. A sharp exothermic peak at −20 °C is attributed to T_c and T_c^* is not observed in this W_c. Crystallization of water was observed at the same temperature in both samples with $W_c = 1.71$ and $0.81\,g\,g^{-1}$, however, ΔH_c of $W_c = 1.71\,g\,g^{-1}$ is extraordinarily large.

Fig. 8 shows DSC heating curves measured at 10 °C min^{-1} of the sample with $W_c = 1.71\,g\,g^{-1}$ having cooled at various rates. T_g at −60 °C and T_{cc} at −30 °C are observed although they are not distinct. T_m of the sample with W_c $1.71\,g\,g^{-1}$ is observed at 5 °C, which is higher than that of the samples with $W_c = 0.59$ and $0.81\,g\,g^{-1}$. T_m^* markedly shifts to the low temperature side and was found as a shoulder of the melting peak at 15 °C. ΔH_m^* of the sample with $W_c = 1.71\,g\,g^{-1}$ is small in comparison with that of $W_c = 0.59$ and $0.81\,g\,g^{-1}$.

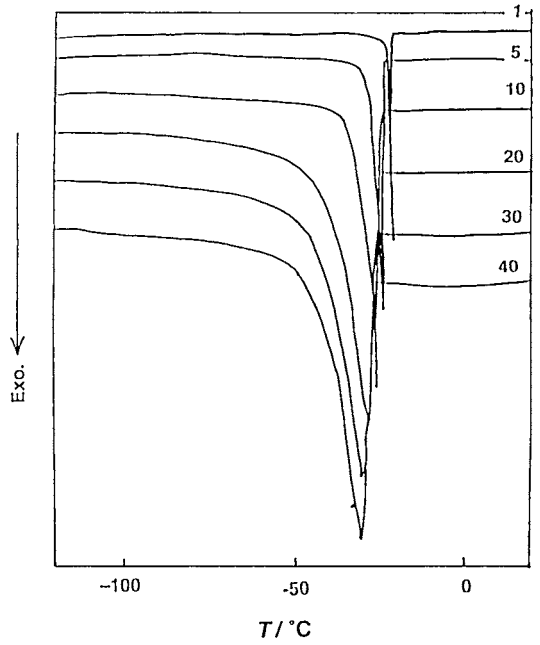

Fig. 7. Stacked DSC cooling curves of various cooling rates of the sample with $W_c = 1.71\,g\,g^{-1}$. Numerals in the figure shows cooling rate.

Relationships between transition temperatures obtained from heating curves and cooling rate are shown in Fig. 9. Melting temperature of water in the system (T_m) and transition temperature from liquid crystalline state to isotropic liquid state (T_m^*) show no cooling rate dependency, but both glass transition temperature (T_g) and cold-crystallization temperature (T_{cc}) decrease with increasing cooling rate. The

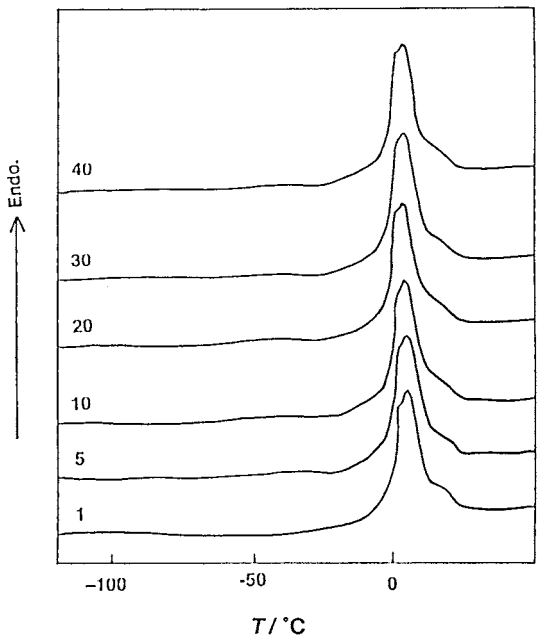

Fig. 8. Stacked DSC heating curves of the sample with $W_c = 1.71\,g\,g^{-1}$ cooled from 50 to −150 °C at various cooling rates. Heating rate = 10 °C min^{-1}.

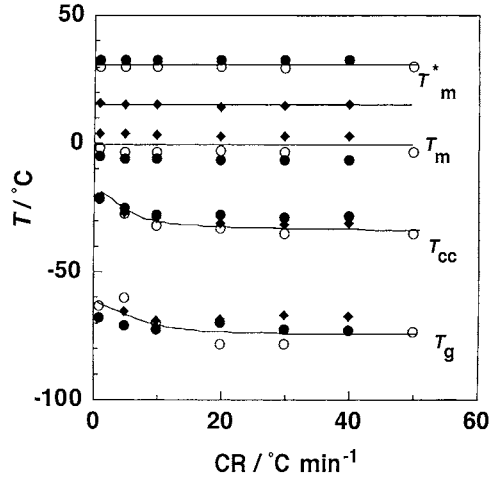

Fig. 9. Relationships between phase transition temperatures and cooling rate of samples having $W_c = 0.59$, 0.81 and $1.71\,g\,g^{-1}$. Heating rate = 10 °C min^{-1}. (●) 0.59, (○) 0.81, (◆) $1.71\,g\,g^{-1}$. T_g: glass transition temperature, T_{cc}: cold-crystallization temperature, T_m: melting temperature, T_m^*: transition temperature from liquid crystalline state to isotropic liquid state in heating.

above results suggest that molecular motion of GG–water systems is markedly affected by structural change of water which varies according to the rate of freezing. The molecular enhancement of GG–water systems at T_g can be detected from ΔC_p values since ΔC_p values depend on the amount of each component and independently obtained ΔC_p values, if the Gordon–Taylor equation is assumed [23].

Fig. 10 shows relationships between ΔC_p values calculated from heating curves and cooling rates of the samples with different W_c. The values of ΔC_p of the samples with $W_c = 0.59$ and $0.81\,g\,g^{-1}$ increased with increasing cooling rate, however, ΔC_p of the sample with $W_c = 1.71\,g\,g^{-1}$ maintains constant values regardless of cooling rate. As shown in the phase diagram of GG–water system shown in Fig. 2, T_m of ice attributing to free water is detected at a W_c higher than $1.3\,g\,g^{-1}$ where T_m value maintains an almost

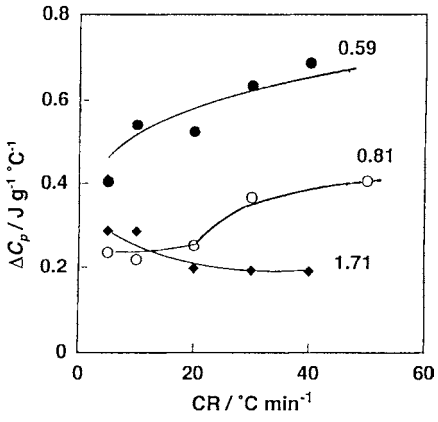

Fig. 10. Relationships between ΔC_p calculated from heating curve and cooling rate of samples having various W_c's: (●) 0.59, (○) 0.81, (◆) $1.71\,g\,g^{-1}$.

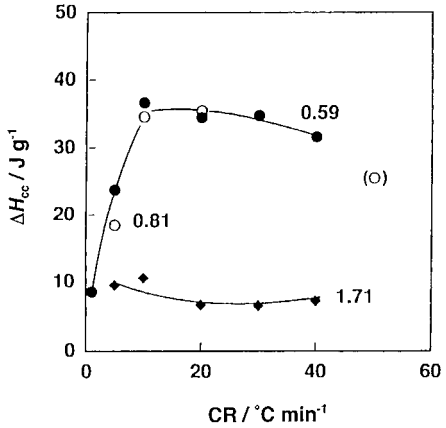

Fig. 11. Relationships between ΔH_{cc} and cooling rate of samples having various W_c's: (●) 0.59, (○) 0.81, (◆) 1.71 g g^{-1}.

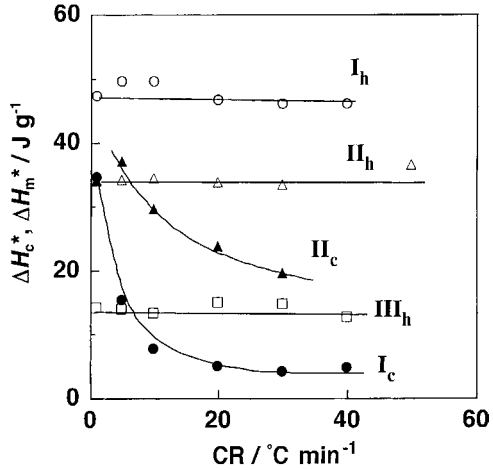

Fig. 12. Comparison of ΔH_m^* and ΔH_c^* of the sample with $W_c = 0.59$, 0.81 and 1.71 g g^{-1} cooled at various cooling rates. (I) 0.59, (II) 0.81, (III) 1.71 g g^{-1}. Suffixes h and c show heating and cooling.

constant value. The fact that ΔC_p decreases with increasing W_c indicates that molecular mobility is restricted in the presence of ice. Moreover, the number of GG molecules associated with non-freezing water decreases with increasing W_c. When non-freezing water molecules which are strongly restricted by polysaccharide molecules via hydrogen bonding are solidified in the glassy state by quenching, amorphous ice is formed. Therefore, it is considered that GG molecules frozen with a large amount of amorphous ice are more mobile and on this account T_g was observed at low temperature and ΔC_p values were large. By rapid cooling, the period required for molecular rearrangement is insufficient and a larger amount of amorphous ice is frozen in the glassy state. When W_c increases, an excess amount of free water forms ice and molecular mobility of GG molecules is restricted by surrounding ice.

As shown in Fig. 9, the starting temperature of cold crystallization decreases with increasing cooling rate. This suggests that molecular rearrangement easily starts when ΔC_p values are large. Fig. 11 shows the relationships between ΔH_{cc} of samples with different water content and cooling rate. When W_c of the systems was 0.59 and 0.81 g g^{-1}, ΔH_{cc} increased in the initial stage, reached about 35 mJ mg^{-1} and then remained at the same value with increasing cooling rate. In contrast, ΔH_{cc} of the sample with $W_c = 1.71$ g g^{-1} remained at ca. 10 J g^{-1} regardless of cooling rate. It is considered that molecular chains associated with amorphous ice are rearranged in the temperature range of cold crystallization. The fact that ΔH_{cc} values increase with increasing cooling rate indicates that the amount of mobile fraction in the system increases by rapid quenching. It is noteworthy that ΔH_{cc} values of samples with $W_c = 0.59$ and 0.81 g g^{-1} are the same. This will be discussed in a later section.

As shown in Fig. 9, transition temperature from liquid crystal to isotropic liquid state, T_m^*, maintains a constant value regardless of cooling rate. Values of transition enthalpy, ΔH_m^*, decrease with increasing W_c, although no cooling rate dependency was found if W_c is constant, as shown in Fig. 12. These results suggest that the liquid crystals are preferentially formed when water molecules in the system are frozen as non-freezing water. With increasing the amount of freezing water, the amount of liquid crystal in the system decreases, suggesting the ice in the system restricts molecular ordering of GG molecules associated with non-freezing water. In contrast to ΔH_m^*, ΔH_c^* markedly depends on cooling rate. ΔH_c^* was not observed when W_c was 0.17 g g^{-1}. Even though ΔH_c^* increases if the sample is cooled at a slow rate, the difference between ΔH_m^* and ΔH_c^* is remarkable, as shown in Fig. 12. It is also seen from this figure that the difference between ΔH_m^* and ΔH_c^* of the sample with $W_c = 0.59$ g g^{-1} is the largest, suggesting the role of non-freezing water.

Almost all water molecules in the GG–water systems with $W_c = 0.59$ g g^{-1} are categorized as non-freezing water [11]. When the above system was cooled from 20 °C, no crystallization of water was observed, as shown in Fig. 3. The exothermic peak observed in DSC cooling curves (Fig. 3) is attributed to liquid crystallization. When cooling rate is low, ΔH_c^* increases in the cooling curve (Fig. 12). This suggests the increase of liquid crystallinity due to sufficient time for molecular reorganization. When the liquid crystallinity increases, molecular enhancement is restricted compared with that of random glassy chains which are obtained by quenching. This can be recognized from the facts that T_g shifts to the high temperature side (Fig. 9) and ΔC_p value decreases (Fig. 10). Furthermore, ΔH_{cc} is considerably low, as shown in Fig. 11. By rapid cooling, GG molecular chains associated with non-freezing water are mainly frozen in the glassy state. Low T_g and large ΔC_p and ΔH_{cc} values indicate that molecular movement starts at T_g and liquid crystallization proceeds at cold crystallization. As shown in Fig. 12, ΔH_m^* values are the same regardless of cooling rate. The liquid crystal is formed in cooling process when cooling rate is low. In heating, the remaining part is frozen as random chains

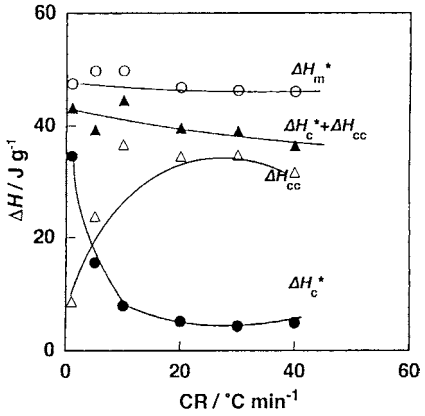

Fig. 13. Comparison of $(\Delta H_c^* + \Delta H_{cc})$ and ΔH_m^* of the sample with $W_c = 0.59\,g\,g^{-1}$ at various cooling rates.

rearrange into liquid crystals. In contrast, the glassy state is formed by rapid cooling and the liquid crystal is formed in heating process via glass transition and cold crystallization. In the case of the samples containing freezing water in addition to non-freezing water, liquid crystallization behaviour is more complex since crystallization of water is accompanied with it. As shown in Fig. 12, the difference between ΔH_m^* and ΔH_c^* decreases for the sample with $W_c = 0.71\,g\,g^{-1}$. In the sample with $W_c = 1.71$, liquid crystallization peak in the cooling curve was masked with crystallization of water and could not detected (Fig. 7).

Based on the above discussion, it is clear that the liquid crystallization takes place in both cooling and heating processes. The comparison was made among ΔH_c^*, ΔH_{cc} and ΔH_m^* for the sample with $W_c = 0.59\,g\,g^{-1}$. Fig. 13 show the relationships between $(\Delta H_c^* + \Delta H_{cc})$ and ΔH_m^* as a function of cooling rate. It is clearly shown that $(\Delta H_c^* + \Delta H_{cc})$ vary in a similar manner to ΔH_m^*. This fact strongly indicates that liquid crystallization occurs at cold crystallization.

From the above results, it is concluded that structural change of water in GG–water system governs the liquid crystallization of the system. It is considered that lyotropic and thermotropic liquid crystals having nematic structure generally observed in water–polysaccharide systems are organized in the same manner as the GG–water system.

References

[1] A.M. Stephen, in: G.O. Aspinall (Ed.), The Polysaccharides, vol. 2, 1983, Chapter 3.
[2] J.K. Seaman, in: R.L. Davidson (Ed.), Handbook of Water-soluble Gums and Resins, McGraw-Hill, New York, 1980, Chapter 6.
[3] J. Kramer, J.T. Uhl, R.K. Prud'homme, Polym. Eng. Sci. 27 (1987) 598.
[4] G. Robinson, S.B. Ross-Murphy, E.R. Morris, Carbohydr. Res. 107 (1982) 17.
[5] P.B. Fernandes, M.P. Goncalves, J.L. Doublier, Carbohydr. Polym. 22 (1933) 99.
[6] E. Costell, M.H. Daasio, L. Izquierdo, L. Duran, Food Hydrocooloids 6 (1992) 275.
[7] K.P. Shatwell, I.W. Sutherland, S.B. Ross-Murphy, I.C. Dea, Carbohydr. Polym. 14 (1991) 115.
[8] S. Kesavan, R.L. Prud'homme, Macromolecules 25 (1992) 2026.
[9] C. Gey, O. Noble, S. Perz, F.R. Tarave, Carbohydr. Res. 173 (1988) 175.
[10] E. Pezron, L. Leibler, A. Ricard, R. Audebert, Macromolecules 21 (1988) 1126.
[11] S. Naoi, T. Hatakeyama, H. Hatakeyama, J. Therm. Anal. Calorim., 70 (2002) 841.
[12] T. Hatakeyama, H. Hatakeyama, W.G. Glasser, H. Hatakeyama (Eds.), Viscoelasticity and Biomaterials, ACS Symposium 489, American Chemical Society, Washington, 1992, p. 329.
[13] T. Hatakeyama, H. Yoshida, H. Hatakeyama, Polymer 28 (1987) 1282.
[14] T. Hatakeyama, H. Yoshida, H. Hatakeyama, Thermochim. Acta 266 (1995) 343.
[15] T. Hatakeyama, K. Nakamura, H. Hatakeyama, Kobunshi Ronbunshu 53 (1996) 795.
[16] F.X. Quinn, T. Hatakeyama, M. Takahashi, H. Hatakeyama, Polymer 35 (1994) 1248.
[17] H. Hatakeyama, T. Hatakeyama, Thermochim. Acta 308 (1998) 3.
[18] T. Hatakeyama, S. Naoi, M. Iijima, H. Hatakeyma, Fibre Preprint (Japan) 55 (2000) 336.
[19] R. Tanaka, T. Hatakeyama, H. Hatakeyama, Polym. Int. 45 (1998) 118.
[20] G.H. Brown, J.J. Wolken, Liquid Crystals and Biological Structure, Academic Press, New York, 1979.
[21] T. Hatakeyama, F.X. Quinn, Thermal Analysis, Wiley, Chichester, 1998.
[22] T. Hatakeyama, Z. Liu, Handbook of Thermal analysis, Wiley, Chichester, 1998, p. 66.
[23] H. Yoshida, Y. Hatakeyama, H. Hatakeyama, W.G. Glasser, H. Hatakeyama (Eds.), Viscoelasticity and Biomaterials, ACS Symposium 489, 1992, p. 217.
[24] B. Wunderlich, J. Phys. Chem. 64 (1960) 1052.
[25] S. Ichihara, Netsu Sokutei no Shinpo (Advance in Thermal Analysis and Calorimetry), vol. 4, Kagaku-gijutsu Pub., Tokyo, 1986, p. 1.
[26] T. Hatekayama, H. Hatakeyama, Thermochim. Acta 267 (1995) 249.